Charge character in the double-barrier quantum dots in well hybrid structure

Wenguo Ning, Weiwei Wang, Xiaobo Jin, Fangmin Guo, Fangyu Yue

Shanghai Key Laboratory of Multidimensional Information Processing, Laboratory of polar Materials and Devices, School of Information Science Technology, East China Normal University, Shanghai, People's Republic of China
E-mail: fmguo@ee.ecnu.edu.cn

Published in Micro & Nano Letters; Received on 18th May 2015; Accepted on 13th July 2015

The charge character in the double-barrier quantum dots (QDs) in a well hybrid structure is investigated experimentally and numerically. The capacitance hysteresis phenomenon of a double-barrier InAs QDs and InGaAs quantum well hybrid structure is reported, as well as the carrier transport properties in the photoelectric device. Due to the coupling effect among multiple QDs, the photoelectric device's measured *I–V* and *C–V* curves show that the capacitance changes with the light intensity. When the dumping readout designed, it can enhance the sensitivity of the device at weak light illumination. This indicates that the photoelectric device has the potential to be a promising candidate both in quantum information applications and highly sensitive imaging applications.

1. Introduction: Electron transfer (ET) from valence to conduction band states in semiconductors is the basis of modern electronics [1–5]. The fundamental process of ET is central to many light-driven reactions. Light-induced ET in molecules starts by excitation to a so-called Franck-Condon electronic excited state, in which non-zero vibrational levels are usually populated [6–10].

Recently, there has been increasing interest in both the electrical and the optical properties of low-dimensional semiconductors. These can restrict carrier transport and transition in at least one dimension (1D) and be used to form the quantum well (QW) and quantum dot (QD) photodetectors using sub-band transition absorption.

QW detectors have a low operating temperature. However, they do not respond to the vertical incident light. The carrier which comes from the sub-band transitions has a short electronic life [11–14]. Quasi-zero-dimensional QD growth has sparked widespread attention, since QDs can be made without dislocation structure in the SK growth mode of the self-assembly. QDs are nanomaterials which are constituted by a small number of atoms. The 3D scale of QDs is 100 nm or less and the internal electronic movement in all directions is subject to quantum confinement. The InAs/GaAs QDs manufactured by self-assembled growth have the advantages of small size, high density, simple fabrication and so on. Owing to the InAs and GaAs being direct band gap semiconductors, which facilitate the easy manufacture of photovoltaic devices, they have become a hot research topic.

Self-assembled III–V QDs are ideally suited for charge transfer devices. They have been widely investigated in the last decade. Their applications in photoelectric and photovoltaic devices such as 1.3 μm laser diodes, infrared photodetectors, and single photon emitters have been demonstrated. In addition to these applications, other advantages of the nanostructures such as the high read/write speed, enhanced capacity for carrier storage, and decent endurance make them a promising candidate for applications of non-volatile memory devices [14, 15].

The QDs which were embedded in the GaAs QW were charged by the electrons from the 2D electron gases. In the detection process, QDs behave as charge traps which can capture photo-generated holes produced in the intrinsic GaAs absorption layer. Especially, the quantum dots-based detector shows a strong 'memory' at illumination. So researchers have tried to apply the InAs QDs and InGaAs QW hybrid structure to perform the write, erase and read operations [2–9].

The photoelectric devices which have a double-barrier InAs QDs and InGaAs QW hybrid structure can make up for the advantage of QDs and the QW and they have shown unique properties such as inner multiplication, lower dark current and high current gains. The devices are promising for application in photodetectors, solar cells and light emitting diodes.

In the work reported in this Letter, we investigated the unique charge character in the double-barrier QDs in well hybrid structure experimentally and numerically. We use the reset technique to dump the stored charge and get the same initial state which cancels the strong 'memory effect' of the QDs. With this process, we systematically study the double-barrier InAs QDs and InGaAs QW hybrid structure and its response wavelength and sensitivity when detecting weak light. The structure's *I–V* and *C–V* properties are calculated numerically using the Crosslight Apsys software.

2. Experimental: The device structure used was grown by molecular beam epitaxy on a n^+-type (100) GaAs substrate. After a 1 μm Si-doped (10^{18} cm^{-3}) GaAs buffer layer and a 30 nm undoped GaAs space, the double barrier structure was deposited in the sequence of the following undoped layers (see [16, 17] for a detailed description of the device composition). On the top, 30 nm undoped GaAs and 30 nm Si-doped (10^{18} cm^{-3}) GaAs were deposited as the capping layer. Ohmic contacts were made both on the top and at the bottom of the device. The spectral responses of the QDs device were measured by Bruker VERTEX 80/80v FTIR spectrometers at room temperature and low temperature (77 K).

The results are shown in Fig. 1. The photoelectric device operated at the wavelength range from 600 to 980 nm. Comparing with spectral responses peaks at different temperatures (300 and 77 K), the spectral responses peaking at 77 K moved to the shorter wavelength. The first spectral response peak appears at about 863 nm. The second peak is at about 910 nm. The third sharp peak is at about 955 nm. The second and third peaks increased much greater than the first peak when the temperature was 77 K. This fact implied that the double-barrier InAs QDs and InGaAs QW hybrid structure enhanced the detection efficiency at low temperature (77K). It also indicated that the photodetector has a broad response spectrum with wavelengths ranging from 100 to 950 nm.

We used the KEITHLEY 4200-SCS and 632.8 nm wavelength laser source to measure the DC characteristic of the photoelectric device at room temperature (300 K) and low temperature (77 K), respectively. Fig. 2 plots the *I–V* characteristics of the photoelectric device under different bias as the light intensity changed. The device showed a great ability to differentiate light power and was not saturated under high power light. The detected optical power

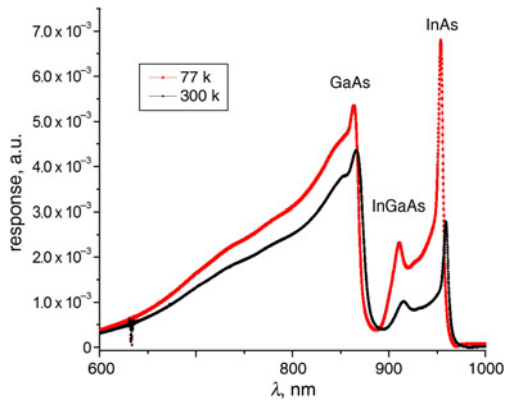

Figure 1 *Spectral responses of the photoelectric device at room temperature and low temperature (77 K)*

range between the minimum and maximum reached about six orders of magnitude. This proved that the photoelectric device has a wide detection range and clear resolution. When the light intensity changed from 50 pW to 1 μW, the photocurrent also increased.

To understand the device detection parameters better, we used formulae (1) and (2) to estimate the detection efficiency and quantum efficiency of the photoelectric device

$$R = \frac{I}{P} \tag{1}$$

$$\eta = \frac{I/e}{P/h\nu} = \frac{Ihc}{Pe\lambda} = R\frac{hc}{e\lambda} = R\frac{1.24}{\lambda(\mu\text{m})} \tag{2}$$

where R is the detection efficiency, I is the photocurrent, P is the laser power and η is the quantum efficiency. When the light power reached 500 pW, the detection efficiency was 0.1588 A/W and the quantum efficiency was 31.11%. Furthermore, the highest detection efficiency could reach 2.73 A/W when the quantum efficiency was 534.79%.

Fig. 3 plots the capacitance hysteresis curve of the photoelectric device in different light intensities at room temperature (77 K). A hysteresis can be shown in comparison of the up-sweeping and down-sweeping C–V curves. This phenomenon occurs at the bias of about −0.75 V. When the light intensity was enhanced, the hysteresis became more obvious. This fact implies that a noticeable amount of electrons has been transferred back and forth by up-sweeping bias and down-sweeping bias [15–18]. The transferred

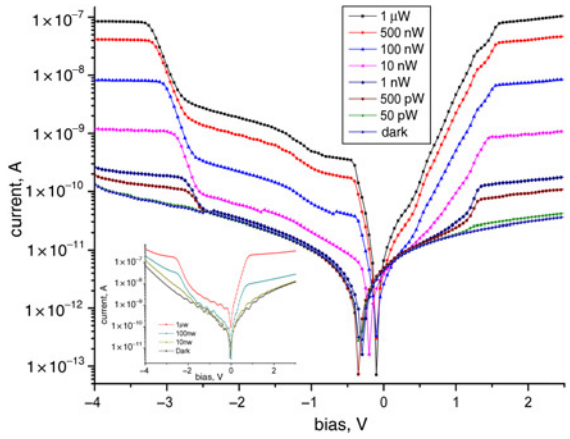

Figure 2 *I–V characteristics of the photoelectric device at room temperature (300 K) and low temperature (77 K)*

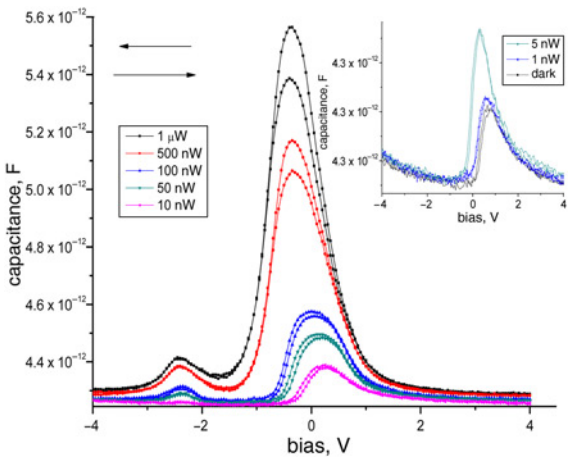

Figure 3 *C–V characteristics of the photoelectric device at room temperature (300 K) by up-sweeping and down-sweeping biases*

electrons are accumulated on the far left side of the X-valley QW of the AlAs layer, while the holes still remain in the Γ-valley GaAs QW. Thus the formed charge polarisation inside the cell structure makes an additional contribution to the capacitance of the photoelectric device. Once the charge polarisation builds up, it should disappear at another bias in the backwards sweeping. Hence, both the space-charge effect and the transferred electrons in the X-valley QW of the AlAs layer, a hysteresis appeared in the measured C–V curves [15–18]. When the was light turned off, the hysteresis still existed.

To study the relationship between the charge storage and sensitivity of the photoelectric device, we used an initial dumped bias when testing the I–V curves of the photoelectric device. The dumping bias changed to −2 V (2 V), and that the I–V curve of the photodetector device from 0 to −1 V (0–1 V). The light intensity was about 3.3 pW (632.8 nm) which used to be difficult to be detected without dumping bias.

The measured results can be seen in Fig. 4. Due to the dumping bias, the photoelectric device showed enhancement of sensitivity. The photocurrent of the photoelectric device increased a lot at −2 V dumping bias. This phenomenon explains that −2 V dumping bias can remove the charge stored in the InAs QD or QW.

The normalised transient photocurrent curves at 77 K are shown in Fig. 5. The sample was illuminated by the chopped laser beam. The chopping frequency was 13 Hz, and the power intensity was

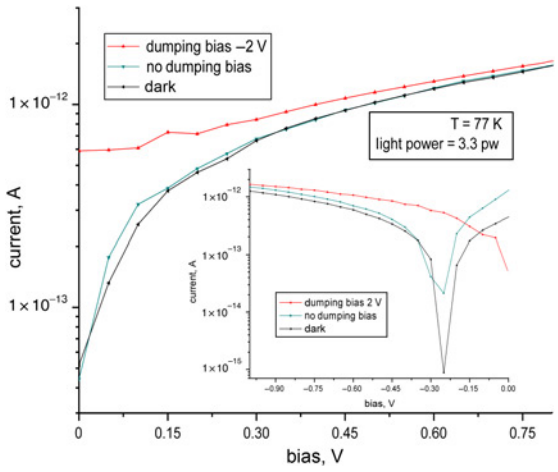

Figure 4 *I–V characteristics of the photodetector device at low temperature (77 K) after −2 V dumping bias*

doi: 10.1049/mnl.2015.0188

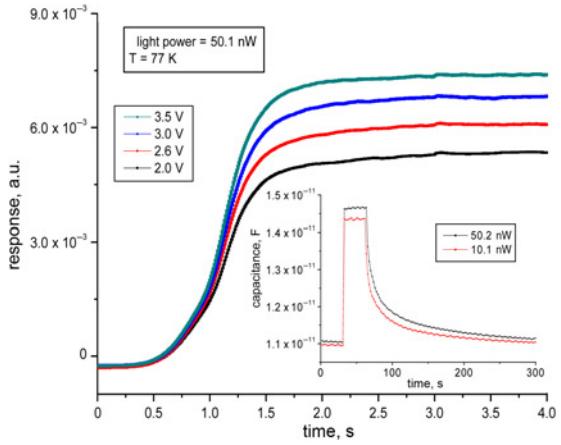

Figure 5 *Normalised transient photocurrent response illuminated by chopped 632.8 nm laser light under different biases and the recovering time of capacitance after different illuminations*

about 50.1 nW. The sample was biased at 3.5, 3.0, 2.6 and 2.0 V. The photocurrent transient from laser-off to laser-on reflects a fast generation process in which electrons and holes were excited and transferred so that they became separated in both real and *K* spaces. The decay transient of the photocurrent from laser-on to laser-off reveals the time that the carrier (electrons and holes) motion, which were stored in the X-valley QW of the AlAs layer and the Γ-valley GaAs-QW, respectively, to recombine either radiatively recombination or non-radiatively recombination [15–18].

Fig. 5 shows the recovering time of the capacitance at 77K. The photoelectric device was illuminated by the power intensities of about 50.2 and 10.1 nW. After the laser turned off, the capacitance of the photoelectric device decreased slowly to the dark capacitance. This process has experienced about 240 s to release the charge stored in the photoelectric device. However, the hysteresis process did not influence the response time of the photoelectric device which was maintain at about 2 ms.

3. Simulation: The device structure was imported into the Crosslight Apsys [19]. More simulation details are given in [20].

The simulation results of the spectral responses of the photoelectric device at room temperature are shown in Fig. 6. There are three peaks about at 870, 900 nm and InAs QD 1400 nm. The first spectral response peak appearing at about 870 nm came from the

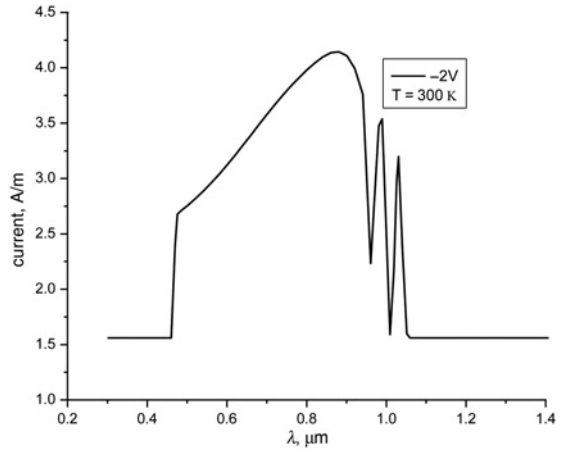

Figure 6 *Photocurrent response spectrum of GaAs QW, InGaAs QW and InAs QD, respectively, at bias voltage of 2 V at room temperature: simulation results*

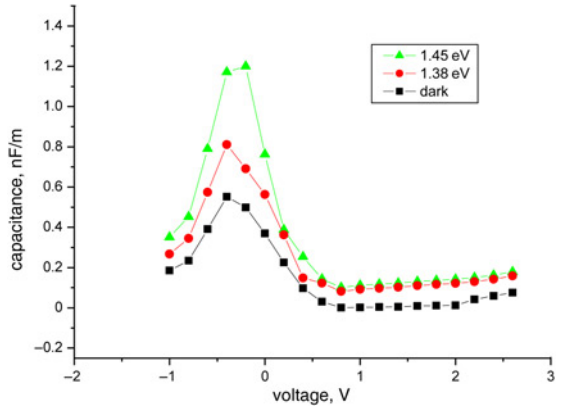

Figure 7 *C–V characteristics of the photoelectric device at room temperature: simulation results*

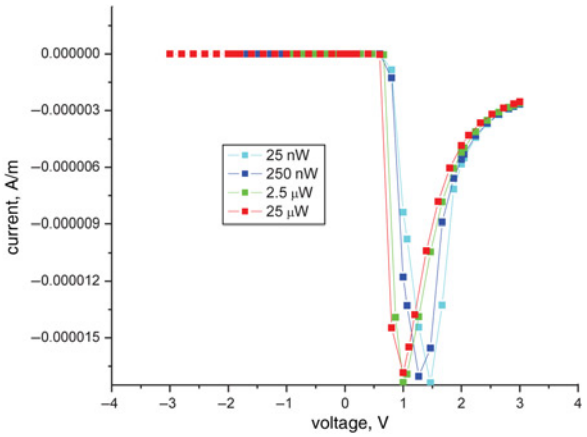

Figure 8 *I–V characteristics of the photoelectric device at room temperature: simulation results*

electron transition of GaAs. The second peak at about 950 nm can be easily attributed to the electron transition of the 6 nm $In_{0.15}Ga_{0.85}$ As QW. The third sharp peak at about 1100 nm came from the photon-absorption of the self-assembled InAs QDs.

Fig. 7 shows the simulation results of the *C–V* characteristics of the photoelectric device at room temperature. The peaks at about −0.5 V agree with the experimental results. This is attributed to the tunnelling photoelectrons in the sub-bands of the QDs and QW.

Fig. 8 shows the simulation results of the *I–V* characteristics of the photoelectric device at room temperature. The zero drift decreases as light power increases. Photo-generated electrons gradually occupy the sub-band. It becomes easier for the electrons in the sub-band with increasing light power [21].

4. Conclusion: The charge character of the double-barrier InAs QDs and InGaAs QW hybrid structure has been investigated experimentally and numerically. We used the dumping bias to enhance the sensitivity and detect the weak light (3.3 pW). We used an initial dumped bias to study the relationship between the charge storage and sensitivity of the photoelectric device. The photoelectric device showed charge storage characteristics after illumination. As a next step, we plan to apply the photoelectric device in various fluorescence tests so as to demonstrate the advantage of the photodetector device with its choice of materials.

5. Acknowledgments: This work was supported by the National Scientific Research Plan (2011CB932903) and the State Scientific and Technological Commission of Shanghai (No. 118014546),

and the State Key Laboratory of Functional Materials for Informatics and Laboratory for terahertz solid state technology Chinese Academy of Science.

6 References

[1] Schultze M., Ramasesha K., Pemmaraju C.D., *et al.*: 'Attosecond band-gap dynamics in silicon', *Science*, 2014, **346**, pp. 1348–1352

[2] Weng Q.C., An Z.H., Xiong D.Y., *et al.*: 'Photocurrent spectrum study of a quantum dot single-photon detector based on resonant tunneling effect with near-infrared response', *Appl. Phys. Lett.*, 2014, **105**, p. 031114

[3] Nowozin T., Narodovitch M., Bonato L., *et al.*: 'Room-temperature hysteresis in a hole-based quantum dot memory structure', *J. Nanotechnol.*, 2013, **2013**, Article id 797964

[4] Komiyama S., Astavief O., Antonov V., *et al.*: 'A single-photon detector in the far infrared range', *Nature (London)*, 2000, **403**, pp. 405–407

[5] Ueda T., Komiyama S., An Z., *et al.*: 'Temperature dependence of charge-sensitive infrared phototransistors', *J. Appl. Phys.*, 2009, **105**, pp. 064517:1–064517:8

[6] Delor M., Scattergood P.A., Sazanovich I.V., *et al.*: 'Toward control of electron transfer in donor-acceptor molecules by bond-specific infrared excitation', *Science*, 2014, **346**, pp. 1492–1495

[7] Wang Z., Komiyama S., Ueda T., *et al.*: 'A modified scheme of charge-sensitive infrared phototransistor', *Appl. Phys. Lett.*, 2009, **95**, pp. 022112:1–022112:3

[8] An Z., Ueda T., Komiyama S., *et al.*: 'Excited states of a closed quantum dot with high sensitivity to infrared photons', *Phys. Rev. B*, 2007, **75**, pp. 085417:1–085417:7

[9] Weng Q.C., An Z.H., *et al.*: 'Electronic-state-controlled reset operation in quantum dot resonant-tunneling single-photon detectors', *Appl. Phys. Lett.*, 2014, **104**, p. 051113

[10] Mao X.W., Gregory C., *et al.*: 'Nanocarbon-based electrochemical systems for sensing, electrocatalysis, and energy storage', *Nano Today*, 2014, **9**, pp. 405–432

[11] Mao L.F.: 'Quantum coupling effects on charging dynamics of nanocrystalline memory devices', *Microelectron. Reliab.*, 2014, **54**, pp. 404–409

[12] Yotter R.A.: 'A review of photodetectors for sensing light-emitting reporters in biological systems', *IEEE Sens. J.*, 2003, **3**, (3), pp. 288–303

[13] Farrell R., Olschner F., Shah K., *et al.*: 'Advances in semiconductor photodetectors for scintillators', *Nucl. Instrum. Methods Phys. Res. A*, 1997, **389**, pp. 194–198

[14] Krishna S., Gunapala S.D., Bandara S.V., *et al.*: 'Quantum dot based infrared focal plane arrays', *Proc. IEEE*, 2007, **95**, (9), pp. 1838–1852

[15] Liao Y.-A., Chao Y.-K., Chang S.-W., *et al.*: 'Memory device application of wide-channel in-plane gate transistors with type-II GaAsSb-capped InAs quantum dots', *Appl. Phys. Lett.*, 2013, **103**, p. 143502

[16] Hu B., Zheng H.Z., Jin P., *et al.*: 'Peculiar photocurrent response due ğd'-X coupling in a GaAs/AlAs heterostructure', *Inst. Phys. Publ.*, 2006, **21**, pp. 643–646

[17] Peng J., Hu B., Hu C.Y., *et al.*: 'Storage of photoexcited electron-hole pairs in an AlAs/GaAs heterostructure created by electron transfer in real and k space', *Chin. Phys. Lett.*, 2002, **19**, (10), pp. 1540–1542

[18] Bian S.B., Tang Y., Li G.R., *et al.*: 'Photon-storage in optical memory cells based on a semiconductor quantum dot-quantum well hybrid structure', *Chin. Phys. Lett.*, 2003, **20**, (8), pp. 1362–1365

[19] http://www.crosslight.com

[20] Wang W.W., Wang M.J., Jin X.B., *et al.*: 'Charge sensitivity simulation on a double barrier GaAs/InGaAs/InAs quantum dot-in-well hybrid structure photodetector', *Opt. Quantum Electron.*, 2015, pp. 1–7

[21] Cui K., Ma W., Zhang Y., *et al.*: 'Forward bias voltage controlled infrared photodetection and electroluminescence from a p-i-n quantum dot structure', *Appl. Phys. Lett.*, 2011, **99**, p. 023502

doi: 10.1049/mnl.2015.0188